MNRAS 000, 1–5 (2016) Preprint 2 March 2016 Compiled using MNRAS LATEX style file v3.0

How much radioactive nickel does ASASSN–15lh require?

Alexandra Kozyreva[1⋆], Raphael Hirschi[1,2],
Sergey Blinnikov[2,3,4], Jacqueline den Hartogh[1]
[1] *Astrophysics group, Keele University, Keele, Staffordshire, ST5 5BG, UK*
[2] *Kavli IPMU (WPI), University of Tokyo, Kashiwa, Chiba 277-8583, Japan*
[3] *ITEP (Kurchatov Institute), Moscow, 117218, Russia*
[4] *VNIIA, Moscow, 127055, Russia*

Accepted XXX. Received YYY; in original form ZZZ

ABSTRACT

The discovery of the most luminous supernova ASASSN–15lh triggered a shock-wave in the supernova community. The three possible mechanisms proposed for the majority of other superluminous supernovae do not produce a realistic physical model for this particular supernova. In the present study we show the limiting luminosity available from a nickel-powered pair-instability supernova. We computed a few exotic nickel-powered explosions with a total mass of nickel up to 1500 solar masses. We used the hydrostatic configurations prepared with the `GENEVA` and `MESA` codes, and the `STELLA` radiative-transfer code for following the explosion of these models. We show that 1500 solar masses of radioactive nickel is needed to power a luminosity of $2 \times 10^{45}\,\mathrm{erg\,s^{-1}}$. The resulting light curve is very broad and incompatible with the shorter ASASSN–15lh time-scale. This rules out a nickel-powered origin of ASASSN–15lh. In addition, we derive a simple peak luminosity – nickel mass relation from our data, which may serve to estimate of nickel mass from observed peak luminosities.

Key words: supernovae: general – supernovae: individual: ASASSN–15lh – stars: massive – stars: evolution – radiative transfer

1 INTRODUCTION

The supernova community is highly excited with the recent discovery of ASASSN–15lh, which is the most luminous supernova ever detected (Dong et al. 2016) among other superluminous supernovae (SLSNe) (see Gal-Yam 2012, for a review). The estimated bolometric luminosity reported is extremely high and reaches $(2.2\pm0.2)\times10^{45}\,\mathrm{erg\,s^{-1}}$. ASASSN–15lh is classified as a Type Ic supernova, so that it requires hydrogen and helium free models to explain it.

As ASASSN–15lh took place close to the host galaxy centre, one of the first possible explanations is that it is a tidal disruption event (TDE, see Supplementary materials in Dong et al. 2016). The detected properties of ASASSN–15lh are different from usual TDEs which generally possess hydrogen and helium (Holoien et al. 2016), although there are at least a few TDEs with a very small amount of hydrogen (Gezari et al. 2015; Kochanek 2016).

One of the most promising models is a rapidly rotating young highly-magnetized neutron star (i.e., a magnetar) powering the supernova ejecta through its dipole radiation (Mazzali et al. 2006; Woosley 2010; Kasen & Bildsten 2010; Metzger et al. 2015, and references therein). In the case of ASASSN–15lh, the magnetar requires a period of 1–2 ms, magnetic field of $0.3–1\times10^{14}$ G, and mass of the ejecta of $6\,M_\odot$ (Bersten et al. 2016), or 0.7 ms, 2.5×10^{13} G, and $8.3\,M_\odot$ (Sukhbold & Woosley 2016). We discuss in more detail the magnetar model in Section 4.

Considering ASASSN–15lh as an interaction-powered supernova seems irrelevant as it would require the collision of very massive hydrogen–helium poor shells and very high energies (Chevalier & Irwin 2011; Ginzburg & Balberg 2012; Moriya et al. 2013; Baklanov et al. 2015; Sorokina et al. 2015). Varying parameters (e.g. mass of the shell or energy) in the interaction model allows one to construct an appropriate fit for a given SLSN (Chatzopoulos et al. 2013). However, interaction-powered events have lower photospheric velocities (several thousand $\mathrm{km\,s^{-1}}$).

From the stellar evolution point of view, there are a number of ideas as to how the star may produce shells or a dense wind, either hydrogen-free or hydrogen-rich. Either metal-free or metal-rich very massive stars undergo enhanced mass–loss due to pulsations (Yoon & Cantiello 2010; Fadeyev 2011; Moriya & Langer 2015). Luminous blue

⋆ E-mail: a.kozyreva@keele.ac.uk

variables (Humphreys & Davidson 1994) or very massive stars with similar activity are good candidates for producing dense circumstellar environments. Yusof et al. (2013) show that mass-loss rates reach several 10^{-3} M$_\odot$ yr^{-1} during core helium burning phases of 300 – 500 M$_\odot$ rotating and non-rotating models (eWNE phase). The supernova shock smashes into the surrounding medium, and instead of the usual shock breakout the luminous supernova-like event is observed. This is the promising mechanism for Type IIn SNSLe (Moriya et al. 2014), although it remains a parameter–dependent model. Mass-loss can be enhanced by neutrino–emission from the stellar core or waves Meakin & Arnett (2007); Moriya (2014); Shiode & Quataert (2014). Nevertheless, there is no evidence for interaction signatures for ASASSN–15lh from current observations (Milisavljevic et al. 2015).

Pulsational pair-instability supernova is another type of interaction-powered scenario (Woosley et al. 2007). A star with the initial mass below pair-instability supernova (PISN) limit of 140 M$_\odot$ does not explode directly[1] (Woosley & Heger 2015). The star produces a sequence of pulses of explosive nuclear burning caused by pair-creation instability (Yoshida et al. 2016). Eventually it explodes as a normal core-collapse supernova followed by an interaction of supernova ejecta with the previously swept stellar shells (Yan et al. 2015).

The last possible known realistic scenario includes the pair-instability explosion of a very massive star at the upper limit of PISN mass-range ($\sim$ 260 M$_\odot$) (Gal-Yam et al. 2009; Gal-Yam 2012). Heger & Woosley (2002) predict that up to 55 M$_\odot$ of radioactive nickel is generated in this kind of explosion and powers a luminous supernova event.

In the present study we examine the maximum luminosity possible for PISNe. We also examine how much radioactive nickel is needed for ASASSN–15lh, if it is considered to be purely nickel-powered. We describe our toy models in Section 2, discuss the light curves and derive a relation between nickel mass and resulting supernova peak luminosity in Section 3 and 4. We conclude in Section 5.

2 INPUT MODELS AND LIGHT CURVE MODELLING

Our main input models are the following: h200, h200Ni55, 250M, 500M, 750M, 1000M, and 1500M. We summarize their properties important for the current study in Table 1. Our reference model is the h200 model. Its earlier evolution was computed with the stellar evolution code `GENEVA` (Ekström et al. 2012; Yusof et al. 2013). Later evolution and the pair-instability explosion were simulated with the `KEPLER` code (Whalen et al. 2014). This PISN model produces 40 M$_\odot$ of radioactive nickel. To inspect the limiting PISN luminosity (model h200Ni55), we use the h200 model with *artificially* increased, to 55 M$_\odot$, amount of nickel keeping the overall structure as in the original h200 model. We map h200 and h200Ni55 models into the `STELLA` code just before shock breakout to follow up the post-explosion evolution of the h200 and h200Ni55 ejecta (Blinnikov et al. 1998, 2000, 2006; Kozyreva et al. 2014).

As an input for `STELLA` for the other models, we create *artificial* structures in hydrostatic equilibrium. The hydrostatic structures were calculated with the `GENEVA` and `MESA`[2] codes. Fig. 1 presents the density structure of our input models. For their composition, we *artificially* set pure radioactive nickel, leaving a shallow outermost layer consisting of oxygen with a total mass not exceeding 1.7 M$_\odot$. This is done for the numerical stability of the `STELLA` code. The explosion of these toy models in `STELLA` is done manually as an instant (lasting 0.1 s) input of thermal energy spread out up to the surface of the progenitor. The explosion energy mentioned in Table 1 is necessary to initiate the expansion of the progenitor. We chose it as: 120 B (1 B or Bethe = 10^{51} erg), 500 B, 550 B, 700 B, and 600 B for 250M, 500M, 750M, 1000M, and 1500M, respectively.

`STELLA` is a one–dimensional multigroup radiation Lagrangian implicit hydrodynamics code. In the present simulations we use 100 frequency bins. The opacity is calculated

Table 1. Characteristics of PISN models mapped into `STELLA`. Final mass M_{fin} and Ni mass are in solar masses. The energy unit is Bethe (B) which is 10^{51} erg.

model name	M_{fin} [M$_\odot$]	Ni [M$_\odot$]	E_{expl} [B]
h200	131	40	87
h200Ni55	131	55	87
250M	250	249	120
500M	499.9	498.2	500
750M	749.5	748.3	550
1000M	1000	998.8	700
1500M	1500	1499	600

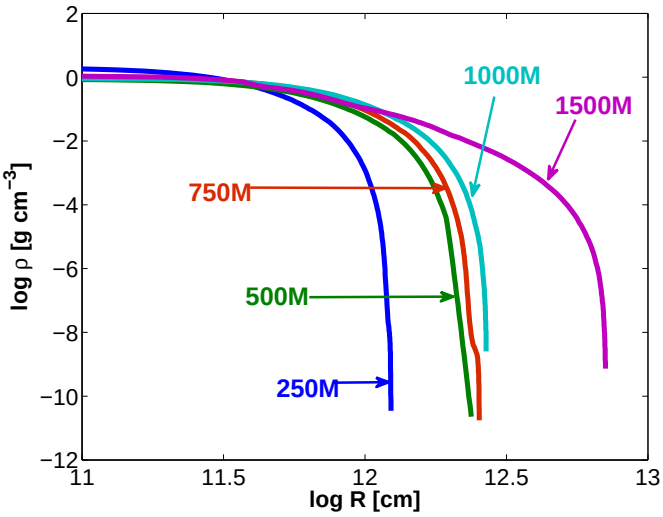

Figure 1. Density structure of models: 250M, 500M, 750M, 1000M, and 1500M.

[1] The initial stellar mass ranges between 100 M$_\odot$ and 140 M$_\odot$ (corresponding CO-core mass lies between 40 M$_\odot$ and 60 M$_\odot$) for progenitors of pulsational pair-instability supernovae.

[2] `Modules for Experiments in Stellar Astrophysics` http://mesa.sourceforge.net/ (Paxton et al. 2011, 2013, 2015).

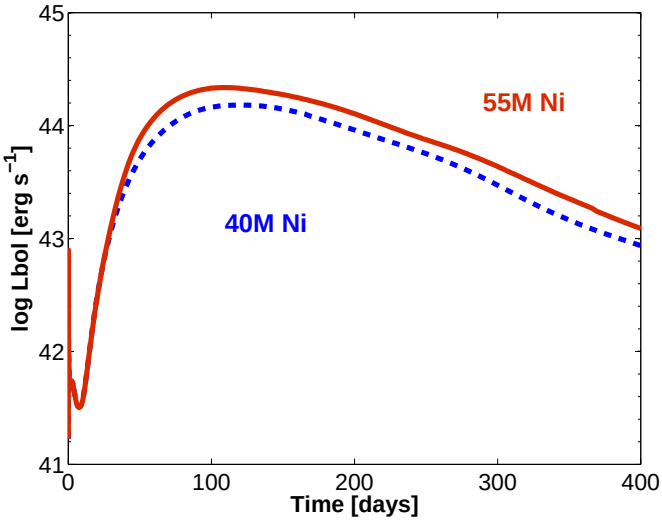

Figure 2. Bolometric light curves of the PISN model h200 with 40 M⊙ of nickel and h200Ni55 with 55 M⊙ of nickel. h200Ni55 demonstrates the PISN limiting luminosity.

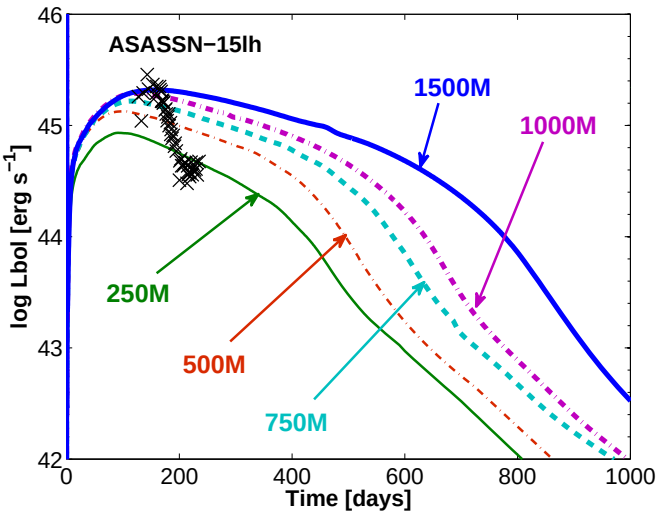

Figure 3. Bolometric light curves of our nickel-rich models: 250M (thin solid), 500M (thin dash-dotted), 750M (thick dashed), 1000M (thick dash-dotted), and 1500M (thick solid). Crosses represent estimated bolometric luminosity of ASASSN–15lh (Dong et al. 2016).

based on about 160,000 spectral lines from Kurucz & Bell (1995) and Verner et al. (1996). Deposition from nickel and cobalt decay is treated in a one-group approximation according to Swartz et al. (1995).

3 RESULTS

We show the comparison between our reference model h200 and the model h200Ni55 in Fig. 2. The peak luminosity of the nickel-powered light curve is expected to depend on the mass of radioactive nickel according to the following relation (Arnett 1979):

$$L_{\rm peak} \sim M_{\rm Ni}\, \varepsilon(t_{\rm peak})\,, \qquad (1)$$

where $\varepsilon(t_{\rm peak})$ is the decay function of nickel and cobalt. In Fig. 2, the difference in the peak luminosity between models with 40 M⊙ and 55 M⊙ of nickel is exactly what Equation 1 predicts and is equal to 0.16 dex. We chose 55 M⊙ of nickel for the h200Ni55 model, as it represents the upper luminosity limit which a PISN is able to produce (Heger & Woosley 2002). Thus, the PISN limit is: peak bolometric luminosity equal to 2.2×10^{44} erg s^{-1}, or a bolometric magnitude of −22.12 mag.

Fig. 3 shows the results for our exotic explosions of progenitors with the following amounts of nickel: ∼250, 500, 750, 1000, and 1500 M⊙. Models reach the following peak luminosities: 8.6×10^{44}, 1.3×10^{45}, 1.7×10^{45}, 1.9×10^{45}, and 2.1×10^{45} erg s^{-1}, respectively. According to Equation 1, 619 M⊙ of nickel supports the peak of ASASSN–15lh. However, we found that our exotic explosions decline from Equation 1 displaying a weaker peak. This happens because nickel is spread out up to the edge of the star, and a large fraction of gamma-photons escape freely without interaction with the ejecta material (Arnett 1979). Hence, the "effective nickel mass" is lower. Fig. 2 from Kozyreva & Blinnikov (2015) also shows that a gradually truncated input model provides a slightly weaker peak even without changing nickel mass.

Fig. 4 illustrates the relation between $L_{\rm peak}$ and $M_{\rm Ni}$ based on results of the current study and other high-mass PISN models[3]. By fitting our data with a linear least-squared fit in Fig. 4, we obtain the following relation:

$$\log L_{\rm peak} = 42.99\,(\pm 0.12) + 0.77\,(\pm 0.05)\,\log M_{\rm Ni}\,. \qquad (2)$$

The relation may be used to estimate the nickel mass needed for a given peak bolometric luminosity, assuming it is a nickel-powered light curve. In addition, SN 1987A (Arnett et al. 1989) and basic SN Ia (W7 model, Nomoto et al. 1984) are included in Fig. 4. The relation given in Eq. 2 resembles that for SNe Ia (Stritzinger & Leibundgut 2005; Blinnikov et al. 2006; Stritzinger et al. 2006).

Based on our simulations, the bolometric luminosity of ASASSN–15lh requires an explosion in which at least 1000 M⊙ of radioactive nickel is produced. It is obvious that there are no known stellar explosions which are capable of generating this huge nickel mass. We discuss a few aspects of producing high nickel mass in Section 4.

A high fraction of nickel results not only in the high peak luminosity, but also in slow evolution of a light curve. The light curve for the 1500M model lasts about 1000 d above 10^{43} erg s^{-1}. This fact resembles the well-known Pskovskii–Phillips relation for SN Ia (Pskovskii 1977; Phillips 1993), i.e., higher mass of nickel supports brighter peak and broader light curve.

[3] Proper PISN explosions: P200, P250 (Ni 18 M⊙, 27 M⊙, Kozyreva et al., in preparation), 250M (Ni 19 M⊙, Kozyreva et al. 2014), "260" (Ni 22 M⊙, Chatzopoulos et al. 2015), h200 (Ni 39 M⊙, Whalen et al. 2014), he130 (Ni 40 M⊙, Kasen et al. 2011). Artificial explosions with artificially increased nickel mass: 55 M⊙ based on h200, 110 M⊙ and 170 M⊙ based on 250M.

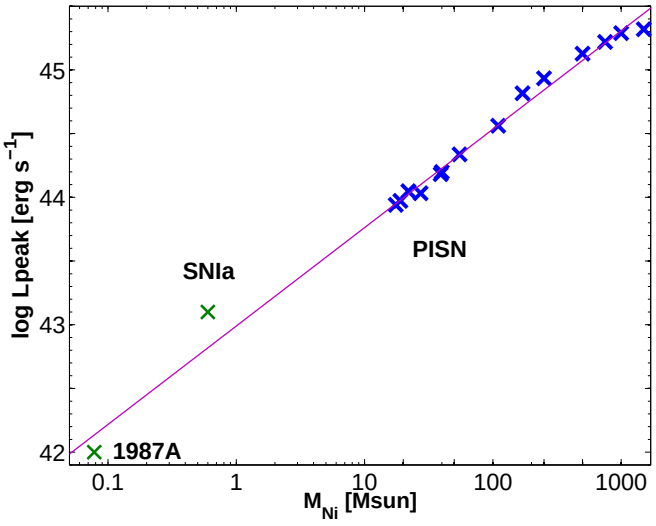

Figure 4. Luminosity – nickel mass relation in the nickel mass range 0.05 – 1500 M⊙. The thin line indicates the least-squared linear fit. SN 1987A and basic SN Ia are superposed.

4 DISCUSSION

In this section we discuss the maximum luminosity for PISN explosions. The grid of models from Heger & Woosley (2002) shows the results of the simulation of non-rotating zero-metallicity models in the helium-core mass range between 65 M⊙ and 135 M⊙. The initial corresponding main-sequence star mass ranges from 140 M⊙ to 260 M⊙. However, the evolutionary parameter space greatly exceeds this grid of very massive stars (Woosley & Heger 2015).

There is no difficulty to produce stars as massive as a thousand solar masses, although they were not observed yet (Wagoner 1969; Abel et al. 2002; Yungelson et al. 2008; Vanbeveren et al. 2009; Hosokawa & Omukai 2009; Hosokawa et al. 2013). Such large stellar objects may be formed in a two-step process through accretion on the already formed proto-star (Kuiper et al. 2011). However, the uncertainty in mass-loss rates for very massive stars implies large uncertainties in their evolution (Vink 2015).

The crucial aspect in the pair-instability explosion is the balance between binding energy of the star and nuclear energy released in the explosive oxygen and silicon burning. Binding energy is proportional to its gravitational energy (with a factor of $\gamma - \frac{4}{3}$), i.e. its mass. For higher massive objects, density is lower, because of radiation-dominated pressure, which leads to larger radii (Fig. 1 in this *Letter*, and Wagoner 1969). A higher mass object is more "spongy", and its specific binding energy (ε/M) is lower (see Table 3 in Bisnovatyi-Kogan & Kazhdan 1967), therefore, it is easy to unbind such systems. Roughly, half of the mass of the star is left after wind mass-loss, and it becomes a carbon-oxygen core (Bond et al. 1982). Once the carbon-oxygen core undergoes the pair-creation instability, oxygen burns and provides the essential fraction of explosive energy, which disrupts the star. The released nuclear energy then depends linearly on the mass of the carbon-oxygen core. Hence, the upper-mass boundary for the pair-instability explosion might be higher than 260 M⊙. It is, however, not expected to reach anywhere near a thousand solar masses of radioactive nickel.

Rotation plays a role in reducing the gravitational force, but not drastically (Fricke 1974). If a carbon-oxygen core retains large angular momentum (Glatzel et al. 1985), the PISN upper-mass boundary may slightly increase.

An object as massive as 500–1000 M⊙ or higher is a subject of general relativity. According to general relativistic effects, these supermassive objects in general collapse into black holes, and nothing prevents contraction. However, some supermassive star models in a narrow mass-range around 55,000 M⊙ explode (see studies by Fricke (1973), Fuller et al. (1986), Johnson et al. (2013), Whalen et al. (2013a), Whalen et al. (2013b), and Chen et al. (2014) which include general relativity), but they do not produce large nickel masses. Adding these factors together cannot help in producing 1000 M⊙ of nickel. Therefore, we conclude that ASASSN–15lh is clearly not a pair-instability explosion.

As we mention in Section 1, if consider a magnetar origin for ASASSN–15lh, the magnetar requires a period of 1–2 ms, magnetic field of $0.3–1\times10^{14}$ G, and mass of the ejecta of 6 M⊙ (Bersten et al. 2016), or 0.7 ms, 2.5×10^{13} G, and 8.3 M⊙ (Sukhbold & Woosley 2016). However, it is not very clear whether a magnetar may store such a high rotational energy (3×10^{52} erg) and strong magnetic field (Metzger et al. 2015). Independent detailed simulations show that if a magnetar powers a supernova ejecta, the resulting event is not luminous (Badjin et al. in preparation). An ambiguous aspect is how the magnetic dipole radiation (a Poynting flux) is converted into thermal energy of the ejecta, as high-energy photons produce electron-positron pairs and, in turn, high gamma-ray opacity (see Kasen et al. 2015, for discussion). This cascading process supplies an uncertainty to the thermalization timescale and thermalization efficiency, and prevents a high photon flux, hence, the production of a luminous supernova. Nevertheless, it may be that independent of our understanding of the microphysics, dipole radiation indeed is converted into ejecta thermal energy, and the magnetar-powered mechanism remains the best candidate for such luminous events.

5 CONCLUSIONS

In the present study we carried out post-explosion evolution of a PISN with a total mass of nickel equal to 55 M⊙. 55 M⊙ of nickel is roughly the upper published limit available in a pair-instability explosion. The limiting bolometric luminosity of a PISN corresponds to 2.2×10^{44} erg s^{-1}, i.e., –22.12 mag. We show that the peak luminosity of ASASSN–15lh significantly exceeds the upper threshold available for PISN explosions, therefore, it is definitely not a PISN.

On top of that we carried out simulations of a grid of exotic explosions with total mass of nickel: 250, 500, 750, 1000, and 1500 M⊙. In the assumption of purely nickel-powered light curves the peak luminosity of 2×10^{45} erg s^{-1} requires at least 1000 M⊙ of nickel. However, the resulting light curve is too broad (1000 d) and incompatible with the shorter time-scale of ASASSN–15lh.

The late-time observations of ASASSN–15lh will shed light on the origin of this unique event. One of the possibilities is that this is a tidal disruption event in which a

companion star firstly loses entirely its hydrogen and helium layers at an earlier time and then accretes on to a massive black hole. Another possible scenario includes a fast rotating highly-magnetized neutron star, although the required rotation and magnetic fields are high.

ACKNOWLEDGEMENTS

The authors acknowledge support from EU-FP7-ERC-2012-St grant 306901. The authors thank Alexander Heger for very useful comments which helped to improve the manuscript. AK thanks Andrea Cristini for proofreading the manuscript. SB is supported by a grant from the Russian Science Foundation (project number 14-12-00203).

REFERENCES

Abel T., Bryan G. L., Norman M. L., 2002, Science, 295, 93
Arnett W. D., 1979, ApJ, 230, L37
Arnett W. D., Bahcall J. N., Kirshner R. P., Woosley S. E., 1989, ARA&A, 27, 629
Baklanov P. V., Sorokina E. I., Blinnikov S. I., 2015, Astronomy Letters, 41, 95
Bersten M. C., Benvenuto O. G., Orellana M., Nomoto K., 2016, preprint, (arXiv:1601.01021)
Bisnovatyi-Kogan G. S., Kazhdan Y. M., 1967, Soviet Ast., 10, 604
Blinnikov S. I., Eastman R., Bartunov O. S., Popolitov V. A., Woosley S. E., 1998, ApJ, 496, 454
Blinnikov S., Lundqvist P., Bartunov O., Nomoto K., Iwamoto K., 2000, ApJ, 532, 1132
Blinnikov S. I., Röpke F. K., Sorokina E. I., Gieseler M., Reinecke M., Travaglio C., Hillebrandt W., Stritzinger M., 2006, A&A, 453, 229
Bond J. R., Arnett W. D., Carr B. J., 1982, in Rees M. J., Stoneham R. J., eds, NATO ASIC Proc. 90: Supernovae: A Survey of Current Research. pp 303–311
Chatzopoulos E., Wheeler J. C., Vinko J., Horvath Z. L., Nagy A., 2013, ApJ, 773, 76
Chatzopoulos E., van Rossum D. R., Craig W. J., Whalen D. J., Smidt J., Wiggins B., 2015, ApJ, 799, 18
Chen K.-J., Heger A., Woosley S., Almgren A., Whalen D. J., Johnson J. L., 2014, ApJ, 790, 162
Chevalier R. A., Irwin C. M., 2011, ApJ, 729, L6
Dong S., et al., 2016, Science, 351, 257
Ekström S., et al., 2012, A&A, 537, A146
Fadeyev Y. A., 2011, Astronomy Letters, 37, 403
Fricke K. J., 1973, ApJ, 183, 941
Fricke K. J., 1974, ApJ, 189, 535
Fuller G. M., Woosley S. E., Weaver T. A., 1986, ApJ, 307, 675
Gal-Yam A., 2012, Science, 337, 927
Gal-Yam A., et al., 2009, Nature, 462, 624
Gezari S., Chornock R., Lawrence A., Rest A., Jones D. O., Berger E., Challis P. M., Narayan G., 2015, ApJ, 815, L5
Ginzburg S., Balberg S., 2012, ApJ, 757, 178
Glatzel W., Fricke K. J., El Eid M. F., 1985, A&A, 149, 413
Heger A., Woosley S. E., 2002, ApJ, 567, 532
Holoien T. W.-S., et al., 2016, MNRAS, 455, 2918
Hosokawa T., Omukai K., 2009, ApJ, 703, 1810
Hosokawa T., Yorke H. W., Inayoshi K., Omukai K., Yoshida N., 2013, ApJ, 778, 178
Humphreys R. M., Davidson K., 1994, PASP, 106, 1025
Johnson J. L., Whalen D. J., Even W., Fryer C. L., Heger A., Smidt J., Chen K.-J., 2013, ApJ, 775, 107
Kasen D., Bildsten L., 2010, ApJ, 717, 245
Kasen D., Woosley S. E., Heger A., 2011, ApJ, 734, 102
Kasen D., Metzger B. D., Bildsten L., 2015, preprint, (arXiv:1507.03645)
Kochanek C. S., 2016, MNRAS,
Kozyreva A., Blinnikov S., 2015, MNRAS, 454, 4357
Kozyreva A., Blinnikov S., Langer N., Yoon S.-C., 2014, A&A, 565, A70
Kuiper R., Klahr H., Beuther H., Henning T., 2011, ApJ, 732, 20
Kurucz R. L., Bell B., 1995, Atomic line list
Mazzali P. A., et al., 2006, Nature, 442, 1018
Meakin C. A., Arnett D., 2007, ApJ, 667, 448
Metzger B. D., Margalit B., Kasen D., Quataert E., 2015, preprint, (arXiv:1508.02712)
Milisavljevic D., James D. J., Marshall J. L., Patnaude D., Margutti R., Parrent J., Kamble A., 2015, The Astronomer's Telegram, 8216
Moriya T. J., 2014, A&A, 564, A83
Moriya T. J., Langer N., 2015, A&A, 573, A18
Moriya T. J., Blinnikov S. I., Baklanov P. V., Sorokina E. I., Dolgov A. D., 2013, MNRAS, 430, 1402
Moriya T. J., Maeda K., Taddia F., Sollerman J., Blinnikov S. I., Sorokina E. I., 2014, MNRAS, 439, 2917
Nomoto K., Thielemann F.-K., Yokoi K., 1984, ApJ, 286, 644
Paxton B., Bildsten L., Dotter A., Herwig F., Lesaffre P., Timmes F., 2011, ApJS, 192, 3
Paxton B., et al., 2013, ApJS, 208, 4
Paxton B., et al., 2015, ApJS, 220, 15
Phillips M. M., 1993, ApJ, 413, L105
Pskovskii I. P., 1977, Soviet Ast., 21, 675
Shiode J. H., Quataert E., 2014, ApJ, 780, 96
Sorokina E., Blinnikov S., Nomoto K., Quimby R., Tolstov A., 2015, preprint, (arXiv:1510.00834)
Stritzinger M., Leibundgut B., 2005, A&A, 431, 423
Stritzinger M., Mazzali P. A., Sollerman J., Benetti S., 2006, A&A, 460, 793
Sukhbold T., Woosley S., 2016, preprint, (arXiv:1602.04865)
Swartz D. A., Sutherland P. G., Harkness R. P., 1995, ApJ, 446, 766
Vanbeveren D., Belkus H., van Bever J., Mennekens N., 2009, Ap&SS, 324, 271
Verner D. A., Verner E. M., Ferland G. J., 1996, Atomic Data and Nuclear Data Tables, 64, 1
Vink J. S., 2015, in Vink J. S., ed., Astrophysics and Space Science Library Vol. 412, Very Massive Stars in the Local Universe. p. 77 (arXiv:1406.5357), doi:10.1007/978-3-319-09596-7_4
Wagoner R. V., 1969, ARA&A, 7, 553
Whalen D. J., Johnson J. L., Smidt J., Heger A., Even W., Fryer C. L., 2013a, ApJ, 777, 99
Whalen D. J., et al., 2013b, ApJ, 778, 17
Whalen D. J., et al., 2014, ApJ, 797, 9
Woosley S. E., 2010, ApJ, 719, L204
Woosley S. E., Heger A., 2015, in Vink J. S., ed., Astrophysics and Space Science Library Vol. 412, Very Massive Stars in the Local Universe. p. 199 (arXiv:1406.5657), doi:10.1007/978-3-319-09596-7_7
Woosley S. E., Blinnikov S., Heger A., 2007, Nature, 450, 390
Yan L., et al., 2015, ApJ, 814, 108
Yoon S.-C., Cantiello M., 2010, ApJ, 717, L62
Yoshida T., Umeda H., Maeda K., Ishii T., 2016, MNRAS, 457, 351
Yungelson L. R., van den Heuvel E. P. J., Vink J. S., Portegies Zwart S. F., de Koter A., 2008, A&A, 477, 223
Yusof N., et al., 2013, MNRAS, 433, 1114

This paper has been typeset from a TEX/LATEX file prepared by the author.